ACS Biomaterials SCIENCE & ENGINEERING

Article

pubs.acs.org/journal/abseba

Interfacially Hydrazone Cross-linked Thermosensitive Polymeric Micelles for Acid-Triggered Release of Paclitaxel

Yang Shi, Cornelus F. van Nostrum, and Wim E. Hennink*

Department of Pharmaceutics, Utrecht Institute for Pharmaceutical Sciences (UIPS), Utrecht University, Universiteitsweg 99, 3508 TB Utrecht, The Netherlands

Supporting Information

ABSTRACT: Polymeric micelles are widely studied as drug carriers, but their poor in vivo stability and, as a consequence, premature drug release hampers their use for targeted drug delivery. Reversible cross-linking of polymeric micelles to achieve stability in the circulation and triggered de-cross-linking/drug release at their site of action is a highly attractive approach to design effective targeted nanomedicines. In this study, the synthesis and RAFT polymerization of a reactive ketone-containing methacrylamide monomer, 1-(acetonylamino)-2-methyl-2-propen-1-one (AMPO), was investigated. A triblock thermosensitive polymer p(HPMAm)-*b*-p(AMPO)-*b*-p(HPMAm-Bz-*co*-HPMAm-Lac) was synthesized by sequential RAFT polymerization of HPMAm for the permanently hydrophilic block, AMPO for the cross-linkable middle block, and HPMAm-Bz with HPMAm-Lac for the thermosensitive block. The triblock copolymer self-assembled into polymeric micelles with size of 52 nm (PDI of 0.03) by increasing the temperature of an aqueous polymer solution above its critical micelle temperature (3 °C). The micelles were subsequently cross-linked after addition of adipic acid dihydrazide, which reacts with the ketone groups of p(AMPO) located at the interfacial region of the micelles. The cross-linked micelles displayed substantially increased thermal and hydrolytic stability as compared to non-cross-linked micelles. The hydrazone bonds in the cross-links were, however, prone to hydrolysis at mild acidic condition (pH 5.0). A chemotherapeutic drug, paclitaxel, was encapsulated in the polymeric micelles with a high loading capacity (29 wt %). The retention of paclitaxel in the micelles at pH 7.4 was substantially increased by interfacial cross-linking, while the release of the drug was triggered at acidic condition (pH 5.0, pH of late endosomes and lysosomes).

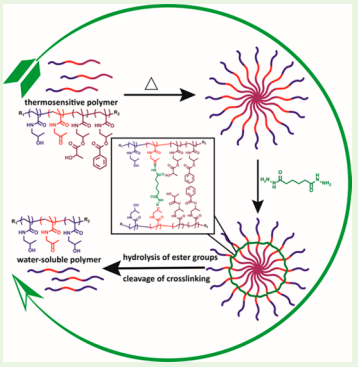

KEYWORDS: *interfacial cross-linking, polymeric micelles, RAFT polymerization, pH sensitive, paclitaxel, triggered release*

1. INTRODUCTION

Amphiphilic block copolymers self-assemble in aqueous solution into polymeric micelles consisting of a hydrophobic core and a hydrophilic shell. The hydrophobic core can accommodate lipophilic drugs and the hydrophilic shell provides so-called "stealth" behavior of these particles after intravenous administration, provided that they have good stability in the blood circulation. Therefore, these systems are currently under extensive investigation as delivery vehicles for hydrophobic drugs,[1−5] and some micellar formulations have reached clinical evaluations.[6,7] Polymeric micelles normally have a size below 100 nm and the diversity of polymers compositions offers opportunities of functionalization, e.g., coupling of targeting ligands.[8−12]

Despite extensive investigations of polymeric micelles for drug delivery, their poor stability in the blood circulation, i.e., premature micellar dissociation associated with drug release, hinders effective delivery of their payloads at aimed sites of action.[13,14] This poor stability is due to the unfavorable shift of the equilibrium between micelles and unimers, in case of massive dilution of the system or removal of the unimers.[15−18]

To prevent dissociation of polymeric micelles in the blood circulation, chemical cross-linking of polymeric micelles is one of the most effective strategies.[15,19−23] Recently, researchers have used reversible reactions for cross-linked polymeric micelles with controlled cross-linking/de-cross-linking behaviors.[24−26] These systems respond to certain internal and/or external stimuli, such as redox potential,[26−28] low pH[29−35] and light,[36,37] to trigger their destabilization and concomitant release of loaded drugs.[38] The ketone-hydrazide nucleophilic addition/elimination reaction is a bioorthogonal reversible reaction that yields stable hydrazone bonds under physiological conditions.[39−42] Interestingly, hydrazone bonds are cleaved at mild acidic conditions, such as the local low pH of late endosomes and lysosomes.[43] Although aldehyde moieties have been applied for cross-linking of polymeric nanoparticles,[44] the present approach distinguishes from this previous study in three aspects. First, ketone groups, instead of more reactive aldehyde moieties, were used. The use of polymers with less reactive ketone groups has advantages because aldehyde groups (in contrast to ketones) might react with, e.g., primary amine groups of proteins.[45] Second, ketones are less prone to oxidation than aldehydes[46] and third, the micellar core of the system described in the present manuscript contains aromatic

Received: January 6, 2015
Accepted: April 29, 2015
Published: April 29, 2015

DOI: 10.1021/acsbiomaterials.5b00006
ACS Biomater. Sci. Eng. 2015, 1, 393−404

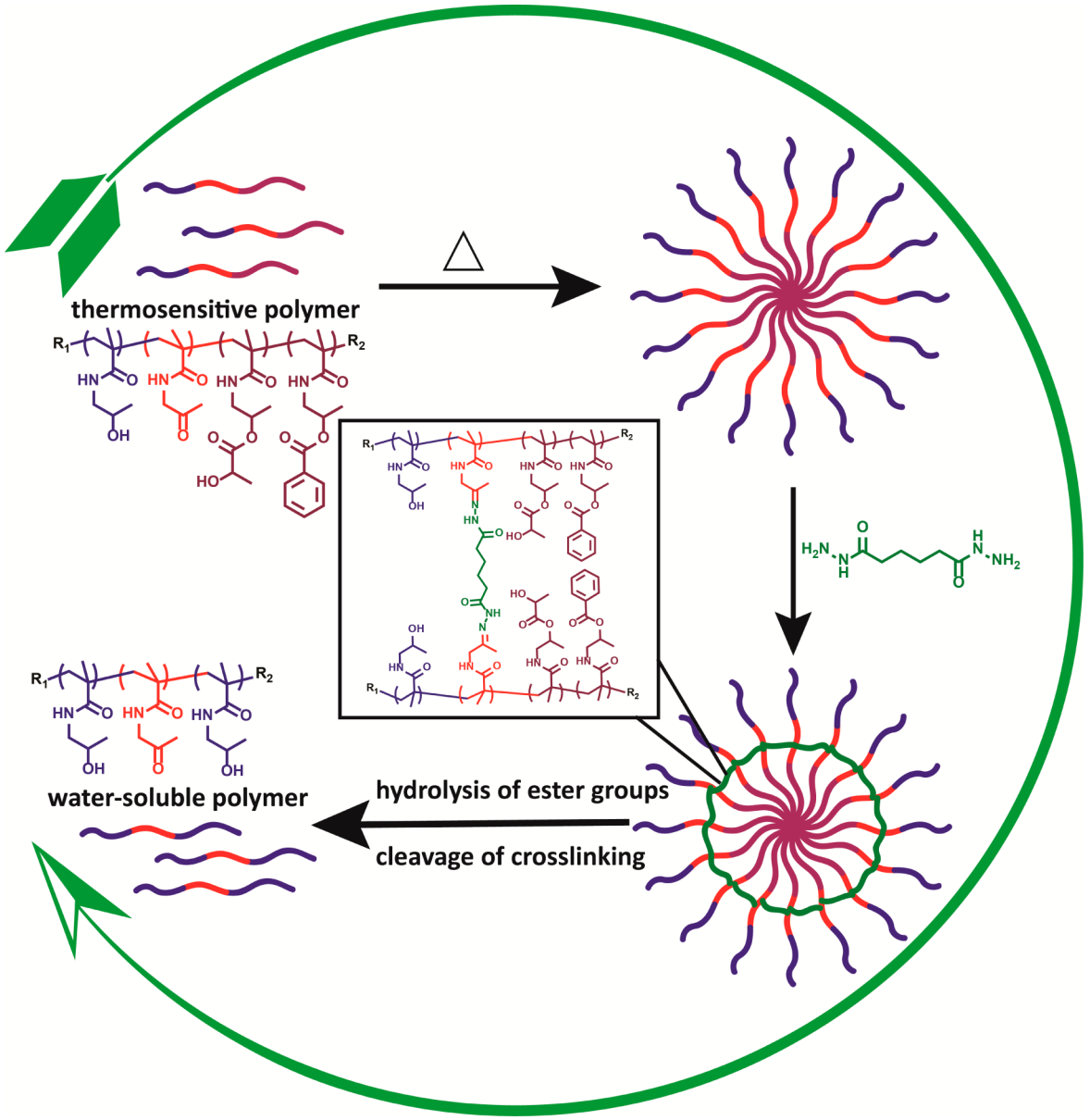

Figure 1. Schematic illustration of formation (upper), cross-linking (right), and destabilization (bottom) of polymeric micelles based on p(HPMAm)-*b*-p(AMPO)-*b*-p(HPMAm-Bz-*co*-HPMAm-Lac).

groups, which positively contribute to the drug loading capacity and drug retention compared to nonaromatic micelles.[47,48]

In the present work, polymeric micelles based on a thermosensitive triblock copolymer providing $\pi-\pi$ stacking due to its aromatic pendent groups in the core of micelles, were cross-linked with hydrazone bonds at the interface between the core and shell of the micelles (Figure 1). Interfacial cross-linking was chosen to avoid intermicellar cross-linking, which may occur with shell-cross-linking and can result in micelle fusion, while core-cross-linking might hamper drug loading and drug integrity.[22] The micellar core is composed of a copolymer of *N*-(2-benzoyloxypropyl) methacrylamide and *N*-(2-hydroxypropyl) methacrylamide monolactate (p(HPMAm-Bz-*co*-HPMAm-Lac) because this core composition has shown to have increased drug loading and retention for aromatic hydrophobic drugs due to $\pi-\pi$ stacking effect.[48] pHPMAm is used for the hydrophilic shell-forming block,[49] which may be a resort to avoid PEGylation related accelerated blood clearance (ABC) effect of nanoparticles in blood circulation when PEG is used as the hydrophilic corona.[44,50,51] For the interfacial segment, a ketone functionalized block of poly(1-(acetonylamino)-2-methyl-2-propen-1-one (p(AMPO)) was incorporated between the thermosensitive hydrophobic block and the hydrophilic block. The three blocks of the polymer were sequentially built in the polymer chain by direct RAFT polymerization,[49,52−54] which is different from previously reported p(HPMAm) containing amphiphilic polymers synthesized by postpolymerization modifications.[55−57] Formation and cross-linking of the polymeric micelles were investigated, and the pH triggered de-cross-linking of and paclitaxel release from the micelles were studied. The effect of empty and PTX-loaded (non)cross-linked polymeric micelles on human umbilical vein endothelial cells (HUVECs) and B16F10 cells were studied in comparison to that of the Taxol vehicle and PTX-containing formulation.

DOI: 10.1021/acsbiomaterials.5b00006
ACS Biomater. Sci. Eng. 2015, 1, 393−404

2. MATERIALS AND METHODS

2.1. Materials. *N*-(2-Hydroxypropyl)methacrylamide (HPMAm) was purchased from Zentiva (Czech Republic). Pyridinium chlorochromate (PCC, 98%), 4-cyano-4-[(dodecylsulfanylthiocarbonyl)-sulfanyl]pentanoic acid (CDTPA), 2,2′-azobis(2-methylpropionitrile) (AIBN, recrystallized twice from methanol before use), and adipic acid dihydrazide (ADH) were ordered from Sigma-Aldrich (Zwijndrecht, The Netherlands). Diethyl ether, hexane (mixture of isomers), ethyl acetate (EtOAc), dimethyl sulfoxide (DMSO) and dichloromethane (DCM) were supplied by Biosolve Ltd. (Valkenswaard, The Netherlands) and used as received. The macro-chain transfer agent (macro-CTA) p(*N*-(2-hydroxypropyl)methacrylamide) (p(HPMAm)) of 4.3 kDa was synthesized according to a previously published method.[49] *N*-(2-Hydroxypropyl) methacrylamide monolactate (HPMAm-Lac) and *N*-(2-benzoyloxypropyl) methacrylamide (HPMAm-Bz) were synthesized and characterized as described previously.[48]

2.2. Synthesis of 1-(Acetonylamino)-2-methyl-2-propen-1-one (AMPO). AMPO was synthesized by oxidation of the hydroxyl group of HPMAm by pyridinium chlorochromate (PCC), following a reported procedure for the synthesis of 1-(carboxyamino)-2-propanone.[58] In detail, a flask was charged with PCC (3 g, 14 mmol) and DCM (14 mL). The flask was immersed in an ice−water bath and HPMAm (1 g in 3 mL DCM, 7 mmol) was added dropwise to the solution with stirring. The mixture was stirred overnight at room temperature, and then 50 mL of diethyl ether was added. The mixture was filtered, the solvent of the filtrate was removed under reduced pressure, and the residual liquid was purified by silica column chromatography with an eluent of hexane/ethyl acetate (3/7, v/v). The final product was obtained as a viscous colorless oil. The structure of the product was confirmed with ^{1}H NMR and electrospray ionization mass spectroscopic analysis (ESI-MS). ^{1}H NMR spectra were recorded using a Gemini 300 MHz spectrometer (Varian Associates Inc. NMR Instruments, Palo Alto, CA) in DMSO-d_6. δ (ppm): 8.2 (s, CO-N$\underline{H}$-CH$_2$), 5.7 and 5.4 (s, C$\underline{H}_2$=C), 3.9 (d, C$\underline{H}_2$-C(CH$_3$)=O), 2.1 (s, C$\underline{H}_3$-C=CH$_2$), 1.8 (s, CH$_2$−C(C$\underline{H}_3$)=O). ESI-MS was performed on a Shimadzu LCMS-QP8000 electrospray ionization mass spectrometer operating in a positive ionization mode.[59]

2.3. RAFT Polymerization of AMPO. p(AMPO) was synthesized by RAFT polymerization according to a procedure that was previously published for the synthesis of p(HPMAm).[49] AIBN was used as the initiator, 4-cyano-4-[(dodecylsulfanyl-thiocarbonyl)sulfanyl]pentanoic acid (CDTPA) was the chain transfer agent (CTA), and the polymerization was performed in DMSO at 70 °C. In brief, a Schlenck tube was charged with the reagents followed by addition of DMSO. The monomer concentration in the resulting solution was 300 mg/mL and the molar ratio of [AMPO]/[CDTPA]/[AIBN] was 1000/5/1. The solution was degassed by three cycles of freeze−vacuum−thaw and the tube was then immersed in a prewarmed oil bath at 70 °C. At predetermined time points, samples (0.1 mL) were withdrawn from the reaction mixture and analyzed by GPC and ^{1}H NMR spectroscopy. The conversion of AMPO was determined by ^{1}H NMR spectroscopy, by comparing the integration areas of resonances from the vinyl protons of AMPO at 5.35 ppm and the protons of methylene group of AMPO at 3.85 ppm.

2.4. RAFT Synthesis of the Triblock Copolymer p(HPMAm)-*b*-p(AMPO)-*b*-p(HPMAm-Bz-*co*-HPMAm-Lac). The triblock copolymer p(HPMAm)-*b*-p(AMPO)-*b*-p(HPMAm-Bz-*co*-HPMAm-Lac) was synthesized by sequential RAFT chain extension of p(HPMAm) macro-CTA with AMPO, followed by chain extension with the comonomers HPMAm-Bz and HPMAm-Lac.[49]

First, p(HPMAm) macro-CTA (4.3 kDa, section 2.1) was extended with AMPO by RAFT polymerization to yield the diblock copolymer p(HPMAm)-*b*-p(AMPO). In detail, a Schlenck tube was charged with p(HPMAm) macro-CTA (38 mg, 0.0088 mmol), AMPO (100 mg, 0.71 mmol), AIBN (0.29 mg, 0.0018 mmol) and DMSO (0.25 mL). The feed molar ratio of [AMPO]/[p(HPMAm)]/[AIBN] was 400/5/1 and the AMPO concentration was 400 mg/mL. The reaction solution was degassed by three cycles of freeze−vacuum−thaw prior to polymerization. Next, the reaction Schlenck tube was immersed in an oil bath at 70 °C. After 4 h, the solution was quenched in liquid nitrogen and subsequently the mixture was thawed at room temperature. The polymer was isolated by precipitation of the reaction mixture in an excess of diethyl ether (repeated two times), redissolved in reverse osmosis (RO) water, and dialyzed against RO water. The polymer was recovered as a pale-yellow powder after freeze-drying.

The triblock copolymer p(HPMAm)-*b*-p(AMPO)-*b*-p(HPMAm-Bz-*co*-HPMAm-Lac) was synthesized by RAFT chain extension of p(HPMAm)-*b*-p(AMPO) with HPMAm-Bz and HPMAm-Lac following the aforementioned procedure as described above in this section. In detail, a Schlenck tube was charged with p(HPMAm)-*b*-p(AMPO) (18 mg, 0.0023 mmol), HPMAm-Bz (22 mg, 0.091 mmol), HPMAm-Lac (78 mg, 0.36 mmol), AIBN (0.074 mg, 0.00045 mmol), and DMSO (0.2 mL). The feed molar ratio of HPMAm-Bz and HPMAm-Lac was 1/4; the feed molar ratio of [HPMAm-Bz and HPMAm-Lac]/[p(HPMAm)-*b*-p(AMPO)]/[AIBN] was 1000/5/1 and the total monomer concentration was 500 mg/mL. The reaction mixture was degassed by three cycles of freeze−vacuum−thaw and then heated at 70 °C in an oil bath. The solution was quenched in liquid nitrogen after 8 h of reaction. The polymer was isolated, purified and dried as described in this section. The characterizations of the synthesized polymers by ^{1}H NMR and GPC are described in section 1 in the Supporting Information.

2.5. Formation and Cross-linking of the Polymeric Micelles. The micelles were prepared by a fast heating method.[48,60] The polymer was dissolved at a concentration of 10 mg/mL at 0 °C for 16 h in phosphate buffer (pH 6.5, 170 mM). Subsequently, micelles were formed in a glass tube containing the polymer solution (typically 1 mL) by immersing the tube in a water bath of 50 °C for 1 min with vigorous shaking. Next, the micellar suspension was cooled to room temperature.

For cross-linking of the polymeric micelles, ADH (= adipic acid dihydrazide, cross-linking agent) was dissolved in the same buffer at a concentration of 50 mg/mL and added to the micellar dispersion at a molar feed ratio of ADH/ketone of 1/2. The micellar suspension was vortexed for 20 s and incubated at 37 °C for 5 h. The size of the (non)cross-linked micelles was measured by dynamic light scattering (DLS) using an ALV-CGS3 system. *Z*-average diameter (Z_{ave}, nm) and polydispersity (PDI) of the micelles are reported. The dispersion of the (non)cross-linked polymeric micelles was freeze-dried and analyzed by Fourier transform infrared spectroscopy (FTIR) using a BIO-RAD FTS6000 FT IR (BIO-RAD, Cambridge, MA, USA) instrument.[61] The particle size and morphology were analyzed by transmission electron microscopy (TEM) using a previously reported method.[48]

2.6. Thermal and Hydrolytic Stability of the (Non)cross-linked Polymeric Micelles. The thermal stability of the (non)cross-linked micelles was studied by monitoring the Z_{ave} and light scattering intensity (LSI) of the micelles by DLS while cooling a micellar dispersion from 25 to 2 °C. The Z_{ave} was plotted against the temperature and the onset on the *x*-axis, obtained by extrapolation of the Z_{ave}−temperatures curve to the baseline, was taken as the CMT (Figure S2).

The hydrolytic stability of (non)cross-linked micelles based on the triblock copolymer was studied by monitoring the Z_{ave} and the LSI of the micelles by DLS under accelerated hydrolysis condition (pH 10.0 and 37 °C) as previously reported.[48] The micelles were prepared and cross-linked as described in section 2.5. The pH of the micellar dispersion was subsequently adjusted to pH 10.0 by a 5-fold dilution with 500 mM Na_2CO_3/$NaHCO_3$ pH 10.0 buffer. The samples were subsequently incubated at 37 °C, and the Z_{ave} and LSI were monitored by continuous DLS measurements for 12−14 h at 37 °C.

DOI: 10.1021/acsbiomaterials.5b00006
ACS Biomater. Sci. Eng. 2015, 1, 393−404

2.7. pH Triggered Destabilization of Hydrazone Coss-linked Micelles. The hydrazone cross-linked micelles prepared as described in section 2.5 were incubated at pH 10.0 and 37 °C as described in section 2.6, to hydrolyze the lactate side groups of the micelles core. The pH of the micellar dispersion was thereafter adjusted to 5.0 by addition of 1 M HCl. The size and light scattering intensity of the micelles at pH 5.0 were measured by DLS at 37 °C.

2.8. Paclitaxel Loading and pH-Dependent PTX Retention in the (Non)cross-linked Polymeric Micelles. To prepare paclitaxel (PTX)-loaded micelles, we added 0.1 mL of PTX solution in ethanol (concentration ranging from 20 to 80 mg/mL) to a glass tube containing 0.9 mL of an ice cold polymer solution of p(HPMAm)-*b*-p(AMPO)-*b*-p(HPMAm-Bz-*co*-HPMAm-Lac) at 10 mg/mL and then immediately heated it for 1 min by immersion of the tube in a water bath at 50 °C. Subsequently, the micellar dispersions were stored overnight at room temperature. The free drug was removed by filtration as reported before[48] and the PTX-loaded polymeric micelles were cross-linked as detailed in 2.5. The PTX content in the micellar dispersion was quantified by UPLC analysis, and the encapsulation efficiency (EE) and loading capacity (LC) were calculated as previously published.[48]

The retention of PTX in the (non)cross-linked micelles was performed as previously reported.[48] PTX-loaded cross-linked micelles were prepared as described above and the pH was adjusted to 7.4 or 5.0 by diluting 5-fold with 500 mM phosphate buffer (pH 7.4) or ammonium acetate buffer (pH 5.0). PTX-loaded non-cross-linked micelles were diluted 5-fold with 500 mM phosphate buffer, pH 7.4. The micellar dispersions were incubated at 37 °C with constant shaking, during which PTX slowly released and precipitated due to its low water solubility (0.3 μg/mL[62]). Aliquots were taken and centrifuged at 5000 g for 10 min to spin down the precipitated drug. Next, the PTX content in the supernatant was quantified by UPLC analysis as described previously.[48]

3. RESULTS AND DISCUSSION

3.1. Synthesis and RAFT Polymerization of AMPO. The synthesis of AMPO was previously reported by Y. Iwakura et al.[63,64] by the classical Schotten−Baumann reaction of methacryloyl chloride and 1-amino-2-propanone hydrochloride in the presence of a base. However, the yield of the reaction was rather low (18%) because of the formation of the byproduct, 2,5-dimethyl-3,6-disubstituted pyrazine. In the present study, AMPO was synthesized by oxidation of *N*-(2-hydroxypropyl) methacrylamide (HPMAm) with pyridinium chlorochromate (PCC) (Scheme 1). The reaction mixture was fractionated by silica column chromatography to obtain the aimed product as a viscous colorless oil with a relatively high yield of 69%. The structure of the product was confirmed by ^{1}H NMR spectroscopy, and ESI-MS (*m*/*z* calculated $[M + H]^+$ 142.08, found 141.90).

Scheme 1. Synthesis and RAFT Polymerization of AMPO

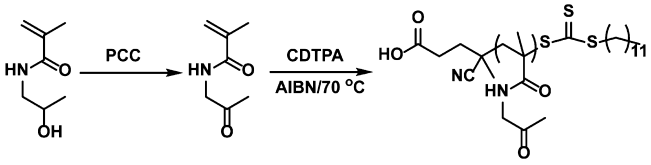

The RAFT polymerization of the AMPO was performed according to a previously reported method for the polymerization of HPMAm to validate the polymerization condition, using AIBN as an initiator and CDTPA as a CTA in DMSO.[49] The semilogarithmic plot of monomer concentration versus time is shown in Figure 2A and shows that the monomer conversion was 53% in 8 h. Figure 2B shows that the experimental M_n of the polymers correlates reasonably well with the theoretical M_n calculated by AMPO conversion, and the molecular weight distribution (PDI) of the polymers was <1.3. Overall, the data show that the RAFT polymerization of AMPO proceeds in a well-controlled manner until 53% conversion of the monomer in 8 h, and control of the polymerization was reduced above this conversion, which can be ascribed by possible side reactions, e.g., irreversible coupling reactions of the radical species.[65]

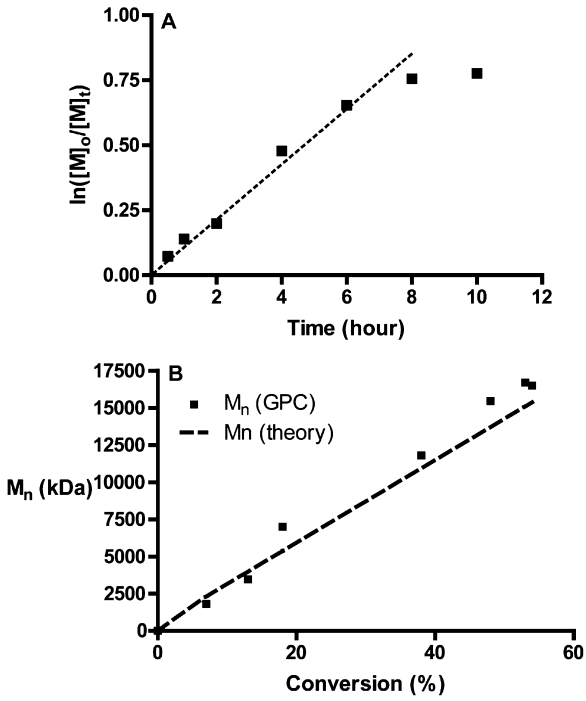

Figure 2. (A) Plot of $\ln([M]_0/[M]_t)$ versus time for the RAFT polymerization of AMPO and (B) plot of experimental M_n (GPC) versus conversion of AMPO with M_n (theory) calculated from the conversion.

Interestingly, previous polymerization of AMPO via free radical polymerization route resulted in a water-insoluble polymer,[64] but the p(AMPO)s synthesized by RAFT in the current study with defined molecular weight ranging from 2 to 15 kDa and low PDI are soluble in water at relatively high concentrations, e.g., 40 mg/mL. The high water-solubility of the p(AMPO)s synthesized by RAFT polymerization can be attributed to the low and narrow distribution of their molecular weight, as compared to those of p(AMPO) synthesized by free radial polymerization (~80 kDa, estimated based on the monomer conversion[64]).

3.2. RAFT Polymerization and Characterizations of Triblock Copolymer p(HPMAm)-*b*-p(AMPO)-*b*-p(HPMAm-Bz-*co*-HPMAm-Lac). The characteristics of the polymers synthesized by RAFT polymerization are shown in Table 1. First, a macro-CTA p(HPMAm) was synthesized by RAFT polymerization with an M_n of 4.3 kDa according to ^{1}H NMR and 3.0 kDa according to GPC (PDI 1.2), which is in the molecular weight range of p(HPMAm) used as a stealth polymer in vivo.[66−68] Subsequently, p(HPMAm) was extended with AMPO (Figure 3A). The AMPO conversion was 34% after a reaction time of 4 h. The resulting diblock copolymer

DOI: 10.1021/acsbiomaterials.5b00006
ACS Biomater. Sci. Eng. 2015, 1, 393−404

Table 1. Characteristics of the Polymers Synthesized by RAFT Polymerization

polymer	M_n (NMR)	M_n (GPC)	PDI
p(HPMAm)	4.3	3.0	1.2
p(HPMAm)-*b*-p(AMPO)	8.1	5.6	1.2
p(HPMAm)-*b*-p(AMPO)-*b*-p(HPMAm-Bz-*co*-HPMAm-Lac)	29.1	22.5	1.4

p(HPMAm)-*b*-p(AMPO) was analyzed by GPC (Figure 3B) and ^{1}H NMR spectroscopy (Figure 3C). From the ^{1}H NMR spectrum, the M_n (by) of the p(AMPO) block, calculated as described in section 2.3, was 3.8 kDa, which ensures a sufficient amount of cross-linkable AMPO repeating units in the polymer. As expected, GPC analysis showed that the retention time of the diblock copolymer was shorter than that of p(HPMAm). The M_n of the diblock copolymer by GPC was 5.6 kDa, which has a reasonable correlation to that calculated by ^{1}H NMR analysis (8.1 kDa). The PDI of the diblock copolymer was low and the same as for the macro-CTA (1.2), which suggests a good control of the chain extension polymerization. Indeed, the GPC trace of the diblock copolymer shows one molecular weight distribution with a negligible low molecular weight tailing, which is a strong evidence that indeed a p(HPMAm)-*b*-p(AMPO) block copolymer was formed.

In the next step, p(HPMAm)-*b*-p(AMPO) was chain extended with HPMAm-Lac and HPMAm-Bz (Figure 3A), which were previously utilized to synthesize the thermosensitive amphiphilic copolymers mPEG-*b*-p(HPMAm-Bz-*co*-HPMAm-Lac).[48] Based on NMR analysis (complete signal assignment is shown in Figure S1), the calculated M_n of the formed triblock copolymer was 29.1 kDa. NMR analysis also showed that the conversions of the both monomers were 48% after 8 h of polymerization and in line herewith the mol % of HPMAm-Bz in the thermosensitive block was 20% which is identical to that of the feed. These data show that HPMAm-Lac and HPMAm-Bz have similar radical polymerization reactivities and were randomly copolymerized, in line with our previous publication.[48] GPC analysis showed that the triblock copolymer has a shorter retention time than that of the diblock copolymer, indicating that chain extension had occurred (Figure 3B). The M_n measured by GPC was 22.5 kDa (PDI of 1.4) (versus 29.1 by ^{1}H NMR) which can be ascribed to the fact that GPC molecular weight is based on PEG standards.[69] Taken together, the results show that a triblock copolymer with defined structure was successfully synthesized by sequential RAFT polymerization.

3.3. Formation and Cross-linking of the Polymeric Micelles. The triblock copolymer is composed of two water-soluble blocks (p(HPMAm) and p(AMPO)) and one thermosensitive block p(HPMAm-Bz-*co*-HPMAm-Lac). Such block copolymers are water-soluble below the lower critical solution temperature (LCST) of the temperature sensitive block and form micelles above this temperature, as shown by Topp et al. for PNIPAM-PEG.[70] Making use of the thermosensitivity of the polymer p(HPMAm)-*b*-p(AMPO)-*b*-p(HPMAm-Bz-*co*-HPMAm-Lac), micelles were "simply" formed by heating an ice-cold aqueous polymer solution of 10 mg/mL to 50 °C. DLS analysis showed that the size of the micelles at 37 °C was 52 nm with a low polydispersity of 0.03.

The polymeric micelles were cross-linked with ADH, which reacts with ketone groups to yield hydrazone bonds (Scheme 2). An attempt of using ^{13}C NMR analysis to quantify the extent of cross-linking was unsuccessful since the signals of the ketone containing block of the micelles could not be detected, which can be explained by their low concentration in combination with the limited mobility of the polymer chains in the polymeric micelles. The cross-linked micelles were analyzed by FTIR spectroscopy (Figure 4A). A typical strong absorption band of ketone groups at 1719 cm^{-1} was observed in the non-cross-linked micelles (blue curve), while this band almost fully disappeared after the cross-linking reaction. This result strongly indicates that the ketone groups of the triblock copolymer had reacted with hydrazide groups of ADH. The IR band of the formed C═N bonds of the imine groups (commonly between 1690 and 1620 cm^{-1})[71] was not clearly visible in the spectrum (in red) which can be ascribed to the fact it does not have a strong IR absorption,[46] and is also masked by neighbor absorption bands, e.g., in this case by the strong band at 1639 cm^{-1} assigned to amide carbonyl of the polymer.[46] To check the integrity of the ester bonds in the HPMAm-Bz-*co*-HPMAm-Lac block during cross-linking, we incubated the closely related block copolymer mPEG-*b*-p(HPMAm-Bz-*co*-HPMAm-Lac)[48] with ADH at the same concentration and reaction conditions, and analyzed with NMR spectroscopy (Supporting Information). Hydroxyl groups of p(HPMAm) repeating units resulted from aminolysis of the ester groups of the p(HPMAm-Bz-*co*-HPMAm-Lac) block were not detected (Figure S2), which suggests that side reactions during the cross-linking of the polymeric micelles based on p(HPMAm)-*b*-p(AMPO)-*b*-p(HPMAm-Bz-*co*-HPMAm-Lac) have not occurred and the reaction was in a chemoselective manner, meaning that only the ketone groups have reacted with ADH.

TEM images of the polymeric micelles before and after cross-linking are shown in Figure 4B, C. The size of the micellar particles is between 30 and 40 nm, which is slightly smaller than the size found by DLS measurement. It should be remarked that DLS reports the *z*-average (Z_{ave}) diameter of the particles, whereas TEM assesses the projected area of the particles which gives an impression of the number-average particle diameter. TEM analysis also shows the polymeric micelles both before and after cross-linking had a spherical shape, which means that, in agreement with the DLS results, interparticle linkage of the micelles had not occur because the reaction was performed in the interfacial zone that is shielded by the hydrophilic p(HPMAm) corona.

The size and polydispersity of the cross-linked micelles (55 nm and 0.04 respectively) were, within experimental error, the same of that of the non-cross-linked micelles. Therefore, intermicellar cross-linking, which would result in an increase in size and PDI, did not occur for the p(HPMAm)-*b*-p(AMPO)-*b*-p(HPMAm-Bz-*co*-HPMAm-Lac) micelles under the applied conditions (10 mg/mL, pH 6.5 and 37 °C).

The size of the micelles measured by DLS was larger than that estimated based on the contour length of polymer chains (38 nm (two times 19 nm, which is the contour length of the polymer calculated according to Utama et al.[72])). This difference can be explained as follows: (1) DLS overestimates the size of the particles.[50] TEM analysis (Figure 4B, C), however, showed that the size of the micelles was between 30 and 40 nm, in agreement with size estimated based on the polymer contour length. (2) The core of thermosensitive polymeric micelles was likely slightly swollen as demonstrated by Soga et al.[73] (3) A small amount of p(HPMAm-Lac-*co*-HPMAm-Bz) might be formed during the polymerization,

DOI: 10.1021/acsbiomaterials.5b00006
ACS Biomater. Sci. Eng. 2015, 1, 393−404

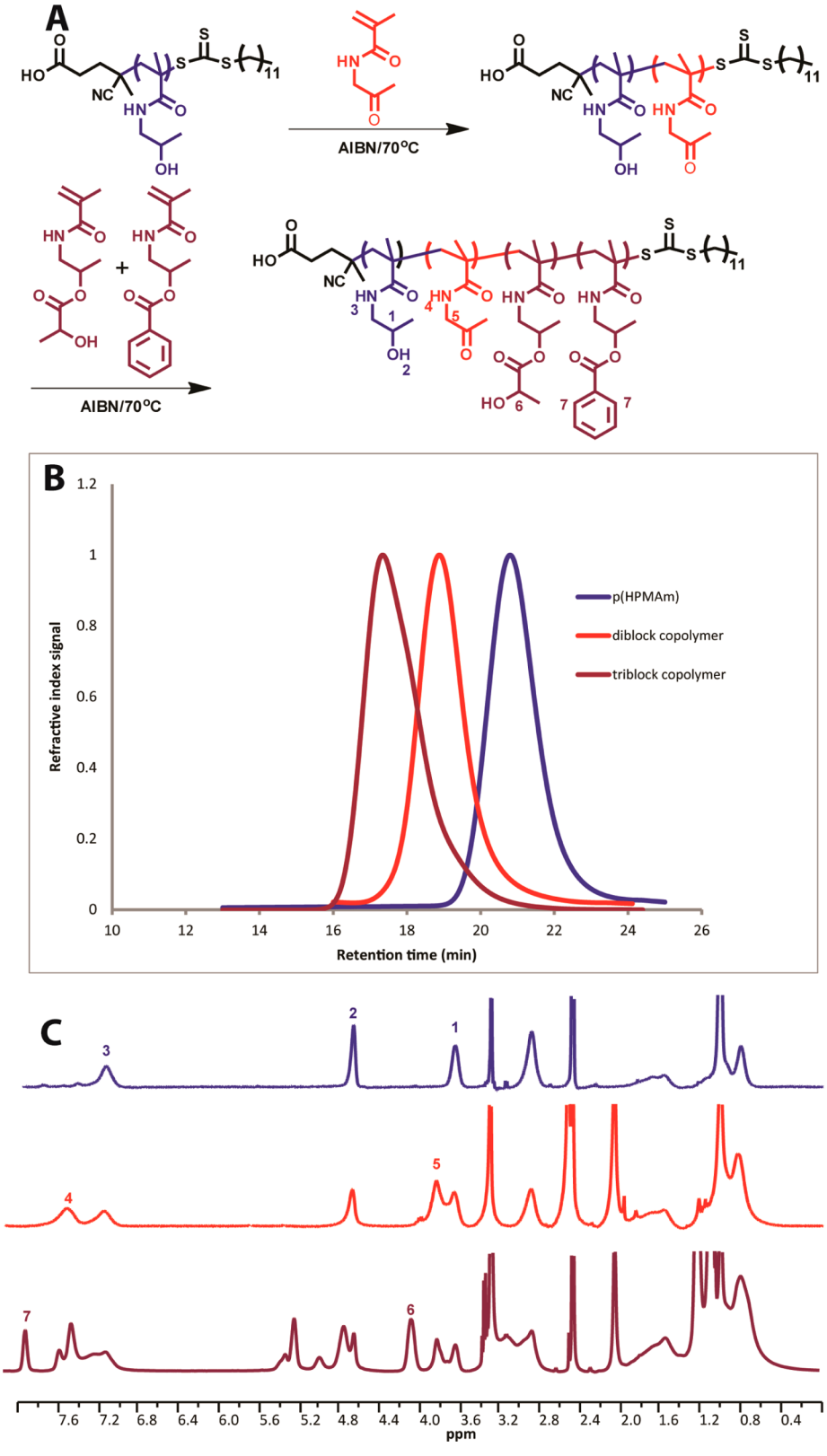

Figure 3. (A) Reaction scheme of the RAFT polymerizations (middle); (B) GPC traces of the macro-CTA p(HPMAm), diblock copolymer p(HPMAm)-*b*-p(AMPO) and triblock copolymer p(HPMAm)-*b*-p(AMPO)-*b*-p(HPMAm-Bz-*co*-HPMAm-Lac); and (C) ^{1}H NMR spectra of p(HPMAm) (in blue) and di/triblock copolymers (in red and purple, respectively).

which because of its hydrophobicity will partition in the core of the micelles and therefore results in an increase in size.

3.4. Thermal and Hydrolytic Stability of the (Non)-cross-linked Polymeric Micelles. Figure 5A shows that when an aqueous dispersion of non-cross-linked micelles was slowly cooled down from 25 to 2 °C, the size of the micelles (55 nm at 25 °C) increased to 65 nm at 5 °C, which indicates swelling of the micellar core caused by hydration of the

DOI: 10.1021/acsbiomaterials.5b00006
ACS Biomater. Sci. Eng. 2015, 1, 393−404

Scheme 2. Cross-linking and De-cross-linking of the Polymeric Micelles Based on p(HPMAm)-*b*-p(AMPO)-*b*-p(HPMAm-Bz-*co*-HPMAm-Lac) at Different pHs

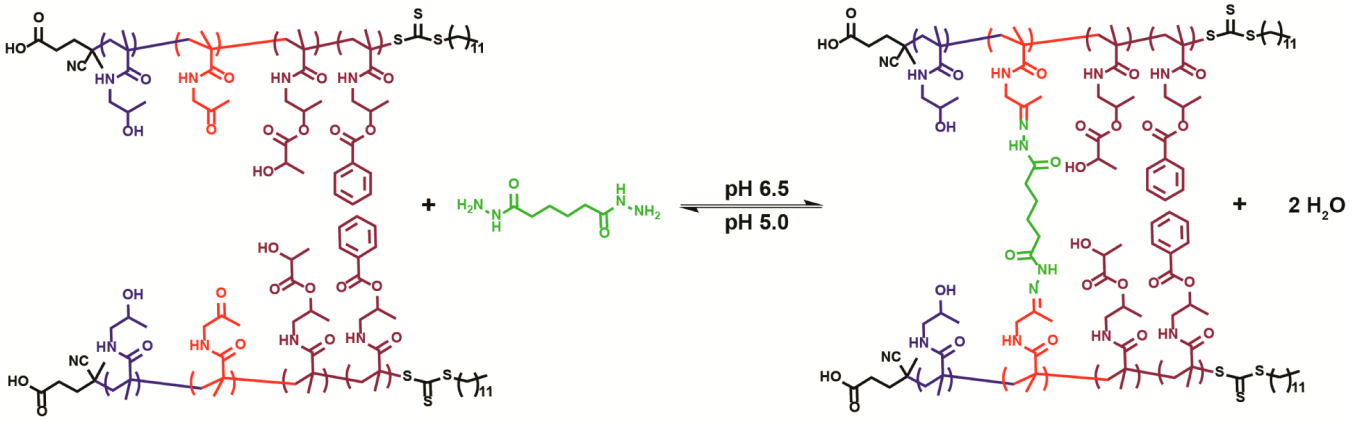

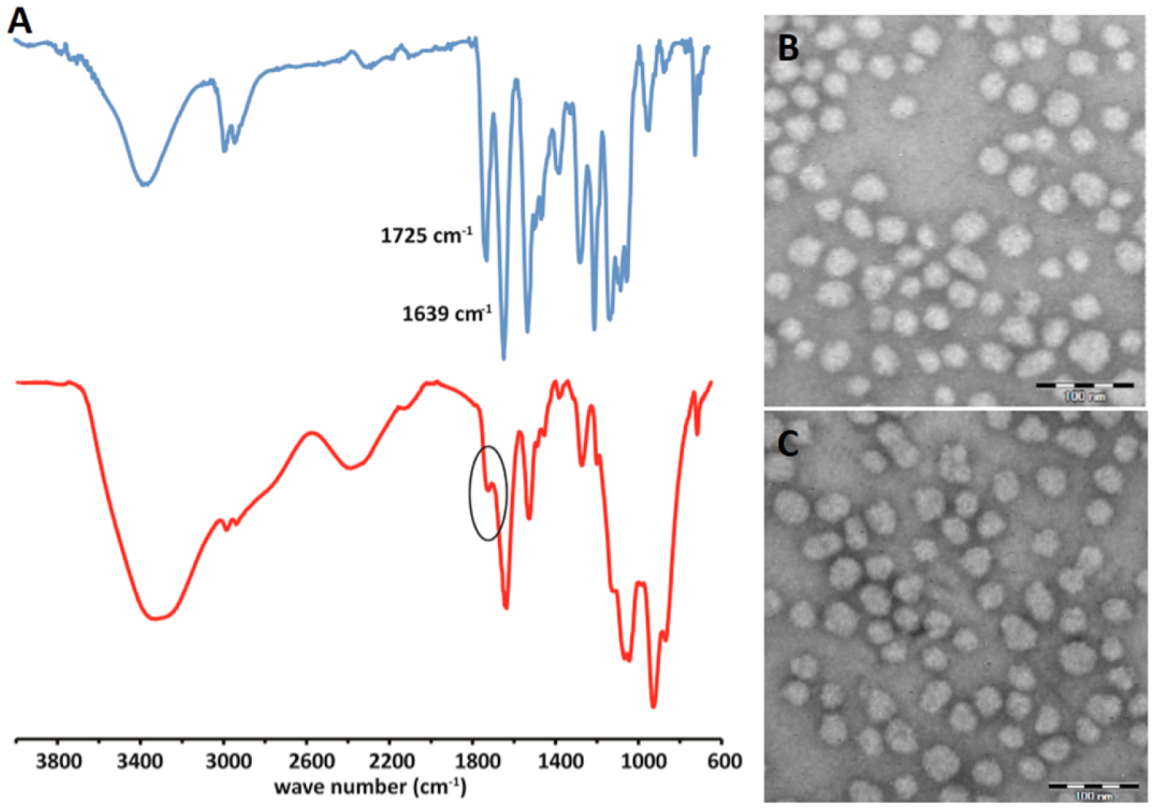

Figure 4. (A) FTIR spectra of the triblock copolymer (in blue) and the cross-linked micelles (in red), TEM images of polymeric micelles (B) before and (C) after cross-linking (scale bar = 100 nm).

p(HPMAm-Bz-*co*-HPMAm-Lac) block. When the temperature further decreased to 2.0 °C, the size dropped to around 5 nm, which was accompanied by a strong decrease in scattering intensity, which indicates that the micelles dissociated.[73] The critical micelle temperature (CMT) of the polymer was around 3 °C (Figure S3). The cross-linked micelles displayed completely different thermoresponsiveness. DLS analysis (Figure 5B) showed that the micelles became slightly bigger (up to around 70 nm) when the dispersion was cooled to around 2 °C, which can be ascribed to the hydration of the cross-linked micellar core at low temperatures. At the same time, the light scattering intensity of the cross-linked micelles decreased by approximately 50% (form 25 to 2.5 °C), because the hydration decreased the density of the micelles. However, no further reduction in scattering intensity, nor a decrease in particle size was observed, as was seen for the non-cross-linked micelles at <5 °C. Therefore, one can conclude that the integrity of the cross-linked micelles was maintained and that the micelles were indeed successfully cross-linked by the hydrazone bonds.

The hydrolytic (in)stability of the (non)cross-linked micelles was conducted under accelerated condition (pH 10.0 and 37 °C). The fact that the hydrolysis of the lactate and benzoate side groups in the pH range 7−10 is first order in [OH^-] allows calculation of the destabilization time of the non-cross-linked polymeric micelles at physiological pH.[74] The non-cross-linked micelles began to swell after around 1 h, accompanied by a gradual but large increase of the light scattering intensity, and

DOI: 10.1021/acsbiomaterials.5b00006
ACS Biomater. Sci. Eng. 2015, 1, 393−404

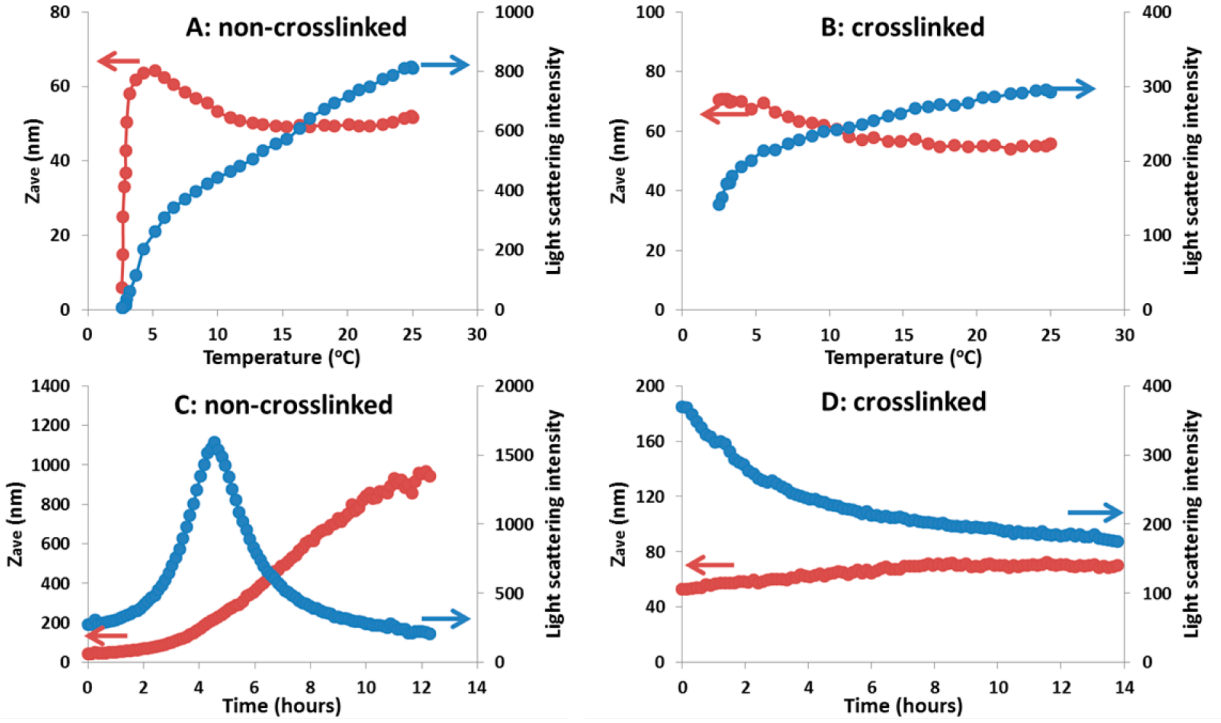

Figure 5. Change of Z_{ave} diameter and light scattering intensity of (non)cross-linked micelles in aqueous medium during cooling ((A) non-cross-linked; (B) cross-linked) and during hydrolysis at pH 10.0 and 37 °C ((C) non-cross-linked; (D) cross-linked) measured by DLS.

dissociated after 4.5 h as reflected by the substantial decrease of the light scattering intensity (Figure 6A). The destabilization

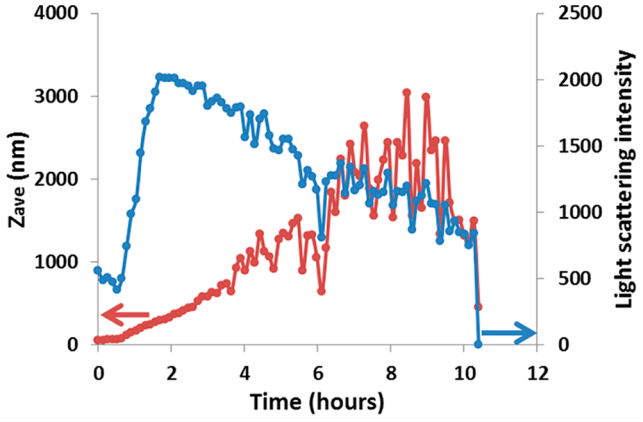

Figure 6. Z_{ave} diameter and light scattering intensity of cross-linked micelles upon incubation at pH 5.0 and 37 °C. Micelles were first subjected to hydrolysis at pH 10 to convert the micellar core from hydrophobic to hydrophilic.

time of the non-cross-linked micelles at pH 7.4 and 37 °C is estimated to be around 1800 h (75 days) based on the first-order hydrolysis kinetics. These data are in line with previous report[48] and can be explained by the hydrolytic removal of the hydrophobic lactate (and benzoate) groups attached to the polymer backbone, followed by hydration of the micellar core due to its increased hydrophilicity. Destabilization of the micelles finally occurs when the LCST of the polymer drops by this increasing hydrophilicity and passes the incubation temperature (37 °C). In contrast to non-cross-linked micelles, the size of the cross-linked micelles only slightly increased during the first 8 h and then the size remained constant for more than 14 h, because hydrazone cross-links are stable at this high pH.[75] Simultaneously, because the size increase was only modest, the light scattering intensity did not increase but decreased, which is likely due to the micellar core becoming less dense and more hydrophilic and hydrated because of hydrolysis of the lactate (and benzoate) side groups. However, the micelles did not disintegrate because of the interfacial cross-linking.

3.5. Acid Hydrolysis of the Polymeric Micelles. As mentioned in the introduction, hydrazone bonds can be cleaved under mild acidic conditions.[75] To investigate this, we took the micelles that were first exposed to pH 10 as described in the previous section, in which the core of the micelles was hydrophilized by hydrolysis of the lactate (and benzoate) groups. DLS analysis was used to investigate the stability of these fully hydrophilic but still cross-linked micelles at 37 °C and pH 5.0, which is the pH value of late endosomes and lysosomes.[76] Figure 6 shows that the light scattering intensity (LSI) and particle size of the micellar dispersion remained quite stable for the first 0.5 h, but then both rapidly started to increase when probably the cross-link density was decreased such that it allowed swelling of the particles. The LSI peaked at close to 2 h and simultaneously the particle size increased from 70 to 370 nm. Beyond 2 h incubation, the LSI decreased, and at 10 h, no particles were detected, which points to acid-catalyzed hydrolysis of the hydrazone bonds in the cross-links of the micelles. DLS measurements showed that both the size and the light scattering intensity of the cross-linked polymeric micelles after hydrolysis and subsequent incubation at pH 5.0 did not change during the first 0.5 h. Thereafter, the size as well as the scattering intensity started to increase, indicating swelling of the micelles due to hydrolysis of the hydrazone linkers. Dissociation of the micelles began after around 3 h of incubation, as reflected by both the dramatic decrease of the size and scattering intensity. The light scattering intensity was

DOI: 10.1021/acsbiomaterials.5b00006
ACS Biomater. Sci. Eng. 2015, 1, 393−404

very low after 10 h of incubation, demonstrating that few micelles were present at that time.

3.6. Preparation, Cross-linking, and Drug-Release of Paclitaxel-Loaded Micelles. Paclitaxel (PTX) was loaded in the polymeric micelles by the fast heating method as described in section 2.8. The results are shown in Figure 7. The

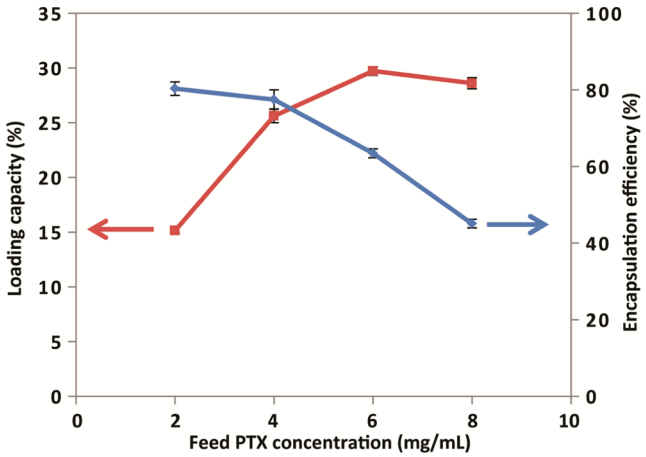

Figure 7. Encapsulation efficiency and loading capacity of the polymeric micelles before cross-linking, with different feed PTX concentrations (polymer concentration of 9 mg/mL).

encapsulation efficiency (EE) decreased from 80 to 45% at increasing feed PTX concentration from 2 to 8 mg/mL. Above a feed of 6 mg/mL, the loading capacity (LC) was 28.6 ± 0.4%, which is in line with previously published data on PTX-loaded micelles with similar core block, i.e., mPEG-*b*-p(HPMAm-Bz-*co*-HPMAm-Lac).[48] The high drug loading capacity and encapsulation efficiency are attributed to the aromatic $\pi-\pi$ stacking between the benzoyl pendent groups in the micellar core and aromatic groups of PTX.[48] The size of the PTX-loaded micelles prepared at a feed PTX concentration of 4 mg/mL was 72 nm (PDI 0.09). The polymeric micelles were then cross-linked with ADH according to section 2.5 and the size of the cross-linked PTX-loaded micelles remained the same after the cross-linking (74 nm, PDI 0.10), as also observed for the nonloaded micelles. The PTX content loss during the cross-linking was negligible, i.e., for micelles with the feed PTX concentration of 4 mg/mL, the PTX content before and after cross-linking were 3.1 ± 0.1 and 3.0 ± 0.1 mg/mL, respectively.

Previous study showed that the mPEG-*b*-p(HPMAm-Bz-*co*-HPMAm-Lac) micelles remain stable at pH 7.4 and 37 °C for at least 30 days,[48] but still released substantial amounts of PTX during the first several days even under nonsink conditions.[48] Likewise, as shown in Figure 8, 45% of PTX was released and precipitated from the non-cross-linked p(HPMAm)-*b*-p(AMPO)-*b*-p(HPMAm-Bz-*co*-HPMAm-Lac) micelles in 10 days at 37 °C. Therefore, the PTX release from both type of micelles with p(HPMAm-Bz-*co*-HPMAm-Lac) based core is mainly attributed to diffusion of PTX in the time frame of the release study. For the interfacially cross-linked micelles at pH 7.4, the drug release rate was significantly retarded (i.e., around 25% in 10 days), which can be explained by the cross-linked interface that gives an additional barrier for diffusion of the PTX molecules. Interestingly, for the PTX-loaded cross-linked micelles incubated at pH 5.0, the drug release rate was similar as that of non-cross-linked micelles at pH 7.4. This accelerated release rate at low pH can be explained by the de-cross-linking

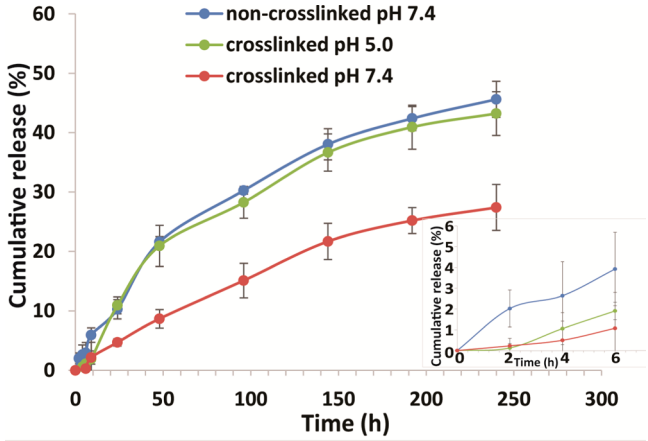

Figure 8. Cumulative PTX release from the non-cross-linked and cross-linked micelles at pH 7.4 and 5.0 and 37 °C. The inset shows the release in the first 6 h.

of the pH sensitive hydrazone linkages as shown in section 3.5. At pH 5.0, the cross-linked micelles were fully de-cross-linked in about 6−10 h as demonstrated in Figure 6, but no hydrolysis of lactate and benzoyl groups occurs under this condition. Thus, the cross-linked micelles were converted into non-cross-linked micelles, which explains the same release of PTX from the non-cross-linked micelles and cross-linked micelles at pH 5.0. This pH-triggered drug release makes the system potentially useful for intracellular drug delivery, in which the drug release is triggered by the low pH of late endosomes and lysosomes.

Under in vivo conditions, because of, e.g., the presence of proteins, the stability of non-cross-linked micelles would likely be too low to retain their integrity and the loaded drug.[15] The main purposes to introduce an acid-degradable cross-linker into the micelles is to maintain in vivo the integrity of the micelles and the retention of the payloads. As shown in Figure 6, the hydrazone bonds in the cross-linked micelles were efficiently cleaved at low pH of, for example, inside late endosomes and lysosomes. Therefore, efficient de-cross-linking of the cross-linked polymeric micelles and drug release from the micelles are expected.

3.7. Effects of Empty and PTX-Loaded Polymeric Micelles on Cell Viability. Cell viability assays were performed using HUVECS and B16F10 cells to assess the cytocompatibility of the (non)cross-linked polymeric micelles as well as that of the Taxol vehicle used in the clinics for PTX, and to determine the in vitro cell killing efficacy of PTX-loaded (non)cross-linked polymeric micelles and the Taxol formulation. Figure 9A shows that the Taxol vehicle (mixture of Cremophor EL and ethanol) substantially affected the viability of HUVECs at a concentration of 0.01 mg/mL, while the cells were fully compatible with the (non)cross-linked polymeric micelle at polymer concentrations up to 0.5 mg/mL. This demonstrates a much better cytocompatibility of the (non)-cross-linked polymeric micelles as compared to the Taxol vehicle. On the other hand, a comparable cytotoxicity of PTX-loaded (non)cross-linked polymeric micelles and the Taxol formulation on B16F10 cells was displayed, which points that the pharmacological effect of PTX was preserved upon encapsulation in the polymeric micelles. PTX encapsulated in the non-cross-linked polymeric micelles could induce a cytotoxic effect following its release from the particles either

DOI: 10.1021/acsbiomaterials.5b00006
ACS Biomater. Sci. Eng. 2015, 1, 393−404

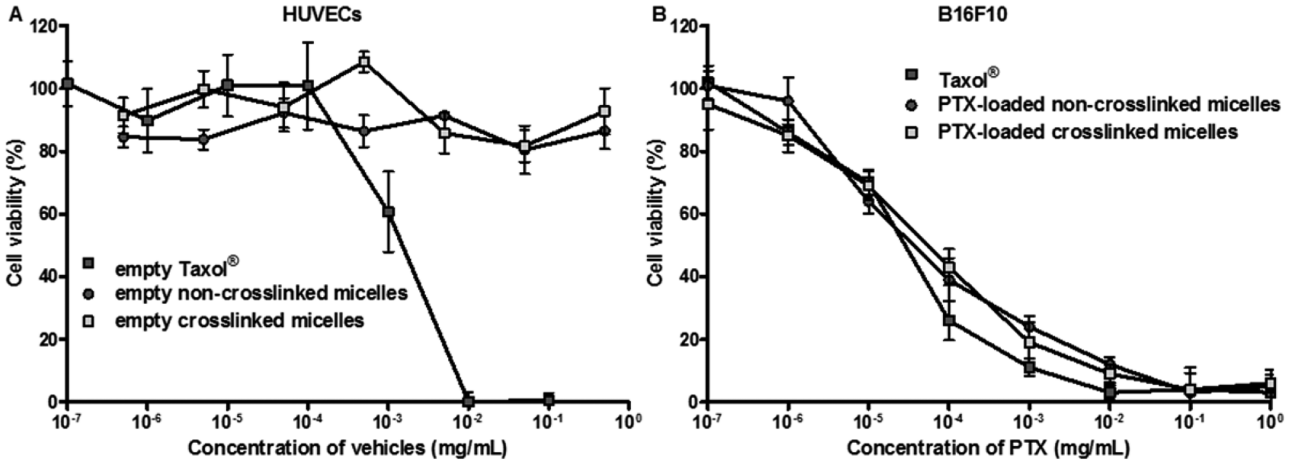

Figure 9. Cytotoxicity of (A) empty and (B) PTX-loaded (non)cross-linked polymeric micelles on (A) HUVECs and (B) B16F10 cells.

extra- or intracellularly. The cytotoxicity of PTX-loaded cross-linked polymeric micelles likely occurs because of the cleavage of the cross-links and accelerated PTX release inside cellular organelles with low pHs as endo/lysozomes.

4. CONCLUSION

A triblock copolymer of p(HPMAm)-*b*-p(AMPO)-*b*-p(HPMAm-Bz-*co*-HPMAm-Lac) was synthesized by RAFT polymerization and the triblock copolymer forms micelles in aqueous solution above 3 °C. The micelles can be interfacially cross-linked by ADH with pH-sensitive hydrazone bonds. These cross-linked micelles were stable at low temperature below the CMT of the non-cross-linked micelles or at high pH, but dissociated at pH 5.0 after the lactate and benzoate groups were hydrolyzed at pH 10.0. PTX-release from the interfacially cross-linked micelles was slower than from non-cross-linked micelles, but can be triggered at pH 5.0. In vitro studies showed that the (non)cross-linked polymeric micelles have a much better safety profile than the Taxol vehicle used in clinics for solubilization of PTX, while the micellar PTX formulations displayed comparable toxicity on B16F10 cells as the Taxol formulation. Further in vivo applications of the present polymeric micelles for drug delivery will be conducted.

■ ASSOCIATED CONTENT

Supporting Information

The Supporting Information is available free of charge on the ACS Publications website at DOI: 10.1021/acsbiomaterials.5b00006.

Characterizations of the synthesized polymers by ^{1}H NMR and GPC, complete signal assignment of ^{1}H NMR spectrum of the triblock copolymer, ^{1}H NMR characterization of mPEG-*b*-p(HPMAm-Bz-*co*-HPMAm-Lac) before and after incubation with ADH, determination of the CMT of p(HPMAm)-*b*-p(AMPO)-*b*-p(HPMAm-Bz-*co*-HPMAm-Lac), and procedure of the in vitro cytotoxicity studies (PDF)

■ AUTHOR INFORMATION

Corresponding Author

*E-mail: W.E.Hennink@uu.nl. Tel.: + 31 30 253 6964. Fax: + 31 30 251 7839.

Notes

The authors declare no competing financial interest.

■ ACKNOWLEDGMENTS

The research was partially supported by China Scholarship Council.

■ REFERENCES

(1) Kataoka, K.; Harada, A.; Nagasaki, Y. Block Copolymer Micelles for Drug Delivery: Design, Characterization and Biological Significance. *Adv. Drug Delivery Rev.* **2001**, *47*, 113−131.
(2) Torchilin, V. P. Micellar Nanocarriers: Pharmaceutical Perspectives. *Pharm. Res.* **2007**, *24*, 1.
(3) Talelli, M.; Rijcken, C. J. F.; van Nostrum, C. F.; Storm, G.; Hennink, W. E. Micelles Based on HPMA Copolymers. *Adv. Drug Delivery Rev.* **2010**, *62*, 231−239.
(4) Gaucher, G.; Marchessault, R. H.; Leroux, J.-C. Polyester-based Micelles and Nanoparticles for the Parenteral Delivery of Taxanes. *J. Controlled Release* **2010**, *143*, 2−12.
(5) Tucker, B. S.; Sumerlin, B. S. Poly(N-(2-hydroxypropyl) methacrylamide)-based Nanotherapeutics. *Polym. Chem.* **2014**, *5*, 1566−1572.
(6) Cabral, H.; Kataoka, K. Progress of Drug-loaded Polymeric Micelles into Clinical Studies. *J. Controlled Release* **2014**, *190*, 465−476.
(7) Matsumura, Y.; Kataoka, K. Preclinical and Clinical Studies of Anticancer Agent-Incorporating Polymer Micelles. *Cancer Sci.* **2009**, *100* (4), 572−579.
(8) Sethuraman, V. A.; Bae, Y. H. TAT Peptide-based Micelle System for Potential Active Targeting of Anti-cancer Agents to Acidic Solid Tumors. *J. Controlled Release* **2007**, *118*, 216−224.
(9) Bae, Y.; Jang, W. D.; Nishiyama, N.; Fukushima, S.; Kataoka, K. Multifunctional Polymeric Micelles with Folate-Mediated Cancer Cell Targeting and pH-Triggered Drug Releasing Properties for Active Intracellular Drug Delivery. *Mol. BioSyst.* **2005**, *1*, 242−250.
(10) Oerlemans, C.; Bult, W.; Bos, M.; Storm, G.; Nijsen, J. F.; Hennink, W. Polymeric Micelles in Anticancer Therapy: Targeting, Imaging and Triggered Release. *Pharm. Res.* **2010**, *27*, 2569−2589.
(11) Lammers, T.; Aime, S.; Hennink, W. E.; Storm, G.; Kiessling, F. Theranostic Nanomedicine. *Acc. Chem. Res.* **2011**, *44*, 1029−1038.
(12) Yang, R.; Meng, F.; Ma, S.; Huang, F.; Liu, H.; Zhong, Z. Galactose-Decorated Cross-Linked Biodegradable Poly(ethylene glycol)-b-poly(ε-caprolactone) Block Copolymer Micelles for Enhanced Hepatoma-Targeting Delivery of Paclitaxel. *Biomacromolecules* **2011**, *12*, 3047−3055.
(13) Owen, S. C.; Chan, D. P. Y.; Shoichet, M. S. Polymeric Micelle Stability. *Nano Today* **2012**, *7*, 53−65.

DOI: 10.1021/acsbiomaterials.5b00006
ACS Biomater. Sci. Eng. 2015, 1, 393−404

(14) Deng, C.; Jiang, Y.; Cheng, R.; Meng, F.; Zhong, Z. Biodegradable Polymeric Micelles for Targeted and Controlled Anticancer Drug Delivery: Promises, Progress and Prospects. *Nano Today* **2012**, *7*, 467−480.
(15) Rijcken, C. J.; Snel, C. J.; Schiffelers, R. M.; van Nostrum, C. F.; Hennink, W. E. Hydrolysable Core-Crosslinked Thermosensitive Polymeric Micelles: Synthesis, Characterisation and In Vivo Studies. *Biomaterials* **2007**, *28*, 5581−5593.
(16) Liu, J.; Zeng, F.; Allen, C. Influence of Serum Protein on Polycarbonate-Based Copolymer Micelles as a Delivery System for A Hydrophobic Anti-cancer Agent. *J. Controlled Release* **2005**, *103*, 481−497.
(17) Lo, C. L.; Huang, C. K.; Lin, K. M.; Hsiue, G. H. Mixed Micelles Formed From Graft and Diblock Copolymers for Application in Intracellular Drug Delivery. *Biomaterials* **2007**, *28*, 1225−1235.
(18) Opanasopit, P.; Yokoyama, M.; Watanabe, M.; Kawano, K.; Maitani, Y.; Okano, T. Influence of Serum and Albumins From Different Species on Stability of Camptothecin-Loaded Micelles. *J. Controlled Release* **2005**, *104*, 313−321.
(19) O'Reilly, R. K.; Hawker, C. J.; Wooley, K. L. Cross-Linked Block Copolymer Micelles: Functional Nanostructures of Great Potential and Versatility. *Chem. Soc. Rev.* **2006**, *35*, 1068−1083.
(20) Bütün, V.; Wang, X. S.; de Paz Báñez, M. V.; Robinson, K. L.; Billingham, N. C.; Armes, S. P.; Tuzar, Z. Synthesis of Shell Cross-Linked Micelles at High Solids in Aqueous Media. *Macromolecules* **1999**, *33*, 1−3.
(21) van Nostrum, C. F. Covalently Cross-Linked Amphiphilic Block Copolymer Micelles. *Soft Matter* **2011**, *7*, 3246−3259.
(22) Read, E. S.; Armes, S. P. Recent Advances in Shell Cross-Linked Micelles. *Chem. Commun.* **2007**, *29*, 3021−3035.
(23) Li, Y.; Lokitz, B. S.; McCormick, C. L. RAFT Synthesis of a Thermally Responsive ABC Triblock Copolymer Incorporating N-Acryloxysuccinimide for Facile in Situ Formation of Shell Cross-Linked Micelles in Aqueous Media. *Macromolecules* **2005**, *39*, 81−89.
(24) Shao, Y.; Huang, W.; Shi, C.; Atkinson, S. T.; Luo, J. Reversibly Crosslinked Nanocarriers for On-demand Drug Delivery in Cancer Treatment. *Ther. Delivery* **2012**, *3*, 1409−1427.
(25) Li, Y.; Xiao, W.; Xiao, K.; Berti, L.; Luo, J.; Tseng, H. P.; Fung, G.; Lam, K. S. Well-Defined, Reversible Boronate Crosslinked Nanocarriers for Targeted Drug Delivery in Response to Acidic pH Values and cis-Diols. *Angew. Chem., Int. Ed.* **2012**, *51*, 2864−2869.
(26) Li, Y.; Xiao, K.; Zhu, W.; Deng, W.; Lam, K. S. Stimuli-Responsive Cross-Linked Micelles for On-demand Drug Delivery Against Cancers. *Adv. Drug Delivery Rev.* **2014**, *66*, 58−73.
(27) Meng, F.; Hennink, W. E.; Zhong, Z. Reduction-Sensitive Polymers and Bioconjugates for Biomedical Applications. *Biomaterials* **2009**, *30*, 2180−2198.
(28) Sun, H.; Guo, B.; Li, X.; Cheng, R.; Meng, F.; Liu, H.; Zhong, Z. Shell-Sheddable Micelles Based on Dextran-SS-Poly(ε-caprolactone) Diblock Copolymer for Efficient Intracellular Release of Doxorubicin. *Biomacromolecules* **2010**, *11*, 848−854.
(29) Talelli, M.; Iman, M.; Varkouhi, A. K.; Rijcken, C. J. F.; Schiffelers, R. M.; Etrych, T.; Ulbrich, K.; van Nostrum, C. F.; Lammers, T.; Storm, G.; Hennink, W. E. Core-Crosslinked Polymeric Micelles with Controlled Release of Covalently Entrapped Doxorubicin. *Biomaterials* **2010**, *31*, 7797−7804.
(30) Bae, Y.; Fukushima, S.; Harada, A.; Kataoka, K. Design of Environment-Sensitive Supramolecular Assemblies for Intracellular Drug Delivery: Polymeric Micelles that Are Responsive to Intracellular pH Change. *Angew. Chem., Int. Ed.* **2003**, *42*, 4640−4643.
(31) Lee, E. S.; Kim, D.; Youn, Y. S.; Oh, K. T.; Bae, Y. H. A Virus-Mimetic Nanogel Vehicle. *Angew. Chem., Int. Ed.* **2008**, *47*, 2418−2421.
(32) Lee, H.; Bae, Y. Brushed Block Copolymer Micelles with pH-Sensitive Pendant Groups for Controlled Drug Delivery. *Pharm. Res.* **2013**, *30*, 2077−2086.
(33) Hrubý, M.; Koňák, Č.; Ulbrich, K. Polymeric Micellar pH-Sensitive Drug Delivery System for Doxorubicin. *J. Controlled Release* **2005**, *103*, 137−148.
(34) Gaitzsch, J.; Appelhans, D.; Wang, L.; Battaglia, G.; Voit, B. Synthetic Bio-Nanoreactor: Mechanical and Chemical Control of Polymersome Membrane Permeability. *Angew. Chem., Int. Ed.* **2012**, *51*, 4448−4451.
(35) Huang, X.; Appelhans, D.; Formanek, P.; Simon, F.; Voit, B. Tailored Synthesis of Intelligent Polymer Nanocapsules: An Investigation of Controlled Permeability and pH-Dependent Degradability. *ACS Nano* **2012**, *6*, 9718−9726.
(36) Jiang, J.; Tong, X.; Zhao, Y. A New Design for Light-Breakable Polymer Micelles. *J. Am. Chem. Soc.* **2005**, *127*, 8290−8291.
(37) Jiang, J.; Qi, B.; Lepage, M.; Zhao, Y. Polymer Micelles Stabilization on Demand through Reversible Photo-Cross-Linking. *Macromolecules* **2007**, *40*, 790−792.
(38) Rapoport, N. Physical Stimuli-Responsive Polymeric Micelles for Anti-Cancer Drug Delivery. *Prog. Polym. Sci.* **2007**, *32*, 962−990.
(39) Prescher, J. A.; Bertozzi, C. R. Chemistry in Living Systems. *Nat. Chem. Biol.* **2005**, *1*, 13−21.
(40) Sletten, E. M.; Bertozzi, C. R. Bioorthogonal Chemistry: Fishing for Selectivity in a Sea of Functionality. *Angew. Chem., Int. Ed.* **2009**, *48*, 6974−6998.
(41) Mahal, L. K.; Yarema, K. J.; Bertozzi, C. R. Engineering Chemical Reactivity on Cell Surfaces Through Oligosaccharide Biosynthesis. *Science* **1997**, *276*, 1125−1128.
(42) Hang, H. C.; Bertozzi, C. R. Ketone Isosteres of 2-N-acetamidosugars as Substrates for Metabolic Cell Surface Engineering. *J. Am. Chem. Soc.* **2001**, *123*, 1242−1243.
(43) Říhová, B.; Etrych, T.; Pechar, M.; Jelínková, M.; Štastný, M.; Hovorka, O.; Kovář, M.; Ulbrich, K. Doxorubicin Bound to a HPMA Copolymer Carrier through Hydrazone Bond Is Effective also in A Cancer Cell Line with a Limited Content of Lysosomes. *J. Controlled Release* **2001**, *74*, 225−232.
(44) Ishihara, T.; Takeda, M.; Sakamoto, H.; Kimoto, A.; Kobayashi, C.; Takasaki, N.; Yuki, K.; Tanaka, K.-i.; Takenaga, M.; Igarashi, R. Accelerated Blood Clearance Phenomenon upon Repeated Injection of PEG-Modified PLA-Nanoparticles. *Pharm. Res.* **2009**, *26*, 2270−2279.
(45) Roberts, M.; Bentley, M.; Harris, J. Chemistry for Peptide and Protein PEGylation. *Adv. Drug Delivery Rev.* **2012**, *64*, 116−127.
(46) Liu, J.; Li, R. C.; Sand, G. J.; Bulmus, V.; Davis, T. P.; Maynard, H. D. Keto-Functionalized Polymer Scaffolds as Versatile Precursors to Polymer Side-Chain Conjugates. *Macromolecules* **2012**, *46*, 8−14.
(47) Shi, Y.; Elkhabaz, A.; Yousef Yengej, F. A.; van den Dikkenberg, J.; Hennink, W. E.; van Nostrum, C. F. Π−Π Stacking Induced Enhanced Molecular Solubilization, Singlet Oxygen Production, and Retention of a Photosensitizer Loaded in Thermosensitive Polymeric Micelles. *Adv. Healthcare Mater.* **2014**, *3*, 2023−2031.
(48) Shi, Y.; van Steenbergen, M. J.; Teunissen, E. A.; Novo, L. s.; Gradmann, S.; Baldus, M.; van Nostrum, C. F.; Hennink, W. E. Π−Π Stacking Increases the Stability and Loading Capacity of Thermosensitive Polymeric Micelles for Chemotherapeutic Drugs. *Biomacromolecules* **2013**, *14*, 1826−1837.
(49) Shi, Y.; van den Dungen, E. T. A.; Klumperman, B.; van Nostrum, C. F.; Hennink, W. E. Reversible Addition−Fragmentation Chain Transfer Synthesis of a Micelle-Forming, Structure Reversible Thermosensitive Diblock Copolymer Based on the N-(2-Hydroxy propyl) Methacrylamide Backbone. *ACS Macro Lett.* **2013**, *2*, 403−408.
(50) Saadati, R.; Dadashzadeh, S.; Abbasian, Z.; Soleimanjahi, H. Accelerated Blood Clearance of PEGylated PLGA Nanoparticles Following Repeated Injections: Effects of Polymer Dose, PEG Coating, and Encapsulated Anticancer Drug. *Pharm. Res.* **2013**, *30*, 985−995.
(51) Szebeni, J. Complement Activation-Related Pseudoallergy Caused by Liposomes, Micellar Carriers of Intravenous Drugs, and Radiocontrast Agents. *Crit. Rev. Ther. Drug Carrier Syst.* **2001**, *18*, 567−606.
(52) Chong, Y. K.; Le, T. P. T.; Moad, G.; Rizzardo, E.; Thang, S. H. A More Versatile Route to Block Copolymers and Other Polymers of

DOI: 10.1021/acsbiomaterials.5b00006
ACS Biomater. Sci. Eng. 2015, 1, 393−404

Complex Architecture by Living Radical Polymerization: The RAFT Process. *Macromolecules* **1999**, *32*, 2071−2074.
(53) Huang, X.; Appelhans, D.; Formanek, P.; Simon, F.; Voit, B. Synthesis of Well-Defined Photo-Cross-Linked Polymeric Nanocapsules by Surface-Initiated RAFT Polymerization. *Macromolecules* **2011**, *44*, 8351−8360.
(54) Stenzel, M. H. RAFT polymerization: An Avenue to Functional Polymeric Micelles for Drug Delivery. *Chem. Commun.* **2008**, *30*, 3486−3503.
(55) Barz, M.; Armiñán, A.; Canal, F.; Wolf, F.; Koynov, K.; Frey, H.; Zentel, R.; Vicent, M. J. P (HPMA)-block-P (LA) Copolymers in Paclitaxel Formulations: Polylactide Stereochemistry Controls Micellization, Cellular Uptake Kinetics, Intracellular Localization and Drug Efficiency. *J. Controlled Release* **2012**, *163*, 63−74.
(56) Barz, M.; Wolf, F. K.; Canal, F.; Koynov, K.; Vicent, M. J.; Frey, H.; Zentel, R. Synthesis, Characterization and Preliminary Biological Evaluation of P (HPMA)-b-p (LLA) Copolymers: A New Type of Functional Biocompatible Block Copolymer. *Macromol. Rapid Commun.* **2010**, *31*, 1492−1500.
(57) Nuhn, L.; Barz, M.; Zentel, R. New Perspectives of HPMA-Based Copolymers Derived by Post-Polymerization Modification. *Macromol. Biosci.* **2014**, *14*, 607−618.
(58) Mai, D. N.; Rosen, B. R.; Wolfe, J. P. Enantioconvergent Synthesis of (+)-Aphanorphine via Asymmetric Pd-Catalyzed Alkene Carboamination. *Org. Lett.* **2011**, *13*, 2932−2935.
(59) Zhang, J.; Kemmink, J.; Rijkers, D. T.; Liskamp, R. M. Cu (I)- and Ru (II)-Mediated "Click" Cyclization of Tripeptides toward Vancomycin-Inspired Mimics. *Org. Lett.* **2011**, *13*, 3438−3441.
(60) Neradovic, D.; Soga, O.; Van Nostrum, C.; Hennink, W. The Effect of the Processing and Formulation Parameters on the Size of Nanoparticles Based on Block Copolymers of Poly (Ethylene glycol) and Poly (*N*-isopropylacrylamide) with and without Hydrolytically Sensitive Groups. *Biomaterials* **2004**, *25*, 2409−2418.
(61) Talelli, M.; Rijcken, C. J.; Lammers, T.; Seevinck, P. R.; Storm, G.; van Nostrum, C. F.; Hennink, W. E. Superparamagnetic Iron Oxide Nanoparticles Encapsulated in Biodegradable Thermosensitive Polymeric Micelles: toward A Targeted Nanomedicine Suitable for Image-Guided Drug Delivery. *Langmuir* **2009**, *25*, 2060−2067.
(62) Ishida, T.; Kiwada, H. Accelerated Blood Clearance (ABC) Phenomenon upon Repeated Injection of PEGylated Liposomes. *Int. J. Pharm.* **2008**, *354*, 56−62.
(63) Iwakura, Y.; Toda, F.; Suzuki, H. Synthesis of N-[1-(1-substituted 2-oxopropyl)]acrylamides and -methylacrylamides. Isolation and Some Reactions of Intermediates of the Dakin-West Reaction. *J. Org. Chem.* **1967**, *32*, 440−443.
(64) Iwakura, Y.; Toda, F.; Suzuki, H. Synthesis and Polymerization of N-[1-(1-substituted-2-oxopropyl)]acrylamides and -methacrylamides. Copolymerization of These Monomers With Styrene and Substituent Effects. *J. Polym. Sci., Part A-1: Polym. Chem.* **1967**, *5*, 1599−1607.
(65) Lowe, A. B.; McCormick, C. L. Reversible Addition−Fragmentation Chain Transfer (RAFT) Radical Polymerization and the Synthesis of Water-Soluble (Co) Polymers under Homogeneous Conditions in Organic and Aqueous Media. *Prog. Polym. Sci.* **2007**, *32*, 283−351.
(66) Barz, M.; Tarantola, M.; Fischer, K.; Schmidt, M.; Luxenhofer, R.; Janshoff, A.; Theato, P.; Zentel, R. From Defined Reactive Diblock Copolymers to Functional HPMA-Based Self-Assembled Nanoaggregates. *Biomacromolecules* **2008**, *9*, 3114−3118.
(67) Koňák, Č. r.; Ganchev, B.; Teodorescu, M.; Matyjaszewski, K.; Kopečková, P.; Kopeček, J. Poly[N-(2-hydroxypropyl)-methacrylamide-block-n-butyl Acrylate] Micelles in Water/DMF Mixed Solvents. *Polymer* **2002**, *43*, 3735−3741.
(68) Lele, B. S.; Leroux, J. C. Synthesis and Micellar Characterization of Novel Amphiphilic A−B−A Triblock Copolymers of N-(2-hydroxypropyl)methacrylamide or N-Vinyl-2-pyrrolidone with Poly-(ε-caprolactone). *Macromolecules* **2002**, *35*, 6714−6723.
(69) Johnson, R. P.; Jeong, Y. I.; Choi, E.; Chung, C. W.; Kang, D. H.; Oh, S. O.; Suh, H.; Kim, I. Biocompatible Poly(2-hydroxyethyl methacrylate)-b-poly(L-histidine) Hybrid Materials for pH-Sensitive Intracellular Anticancer Drug Delivery. *Adv. Funct. Mater.* **2012**, *22*, 1058−1068.
(70) Topp, M.; Dijkstra, P.; Talsma, H.; Feijen, J. Thermosensitive Micelle-Forming Block Copolymers of Poly (ethylene glycol) and Poly (N-isopropylacrylamide). *Macromolecules* **1997**, *30*, 8518−8520.
(71) Furniss, B. S. *Vogel's Textbook of Practical Organic Chemistry*; Pearson Education: Delhi, India, 1989.
(72) Utama, R. H.; Guo, Y.; Zetterlund, P. B.; Stenzel, M. H. Synthesis of Hollow Polymeric Nanoparticles for Protein Delivery via Inverse Miniemulsion Periphery RAFT Polymerization. *Chem. Commun.* **2012**, *48*, 11103−11105.
(73) Soga, O.; van Nostrum, C. F.; Ramzi, A.; Visser, T.; Soulimani, F.; Frederik, P. M.; Bomans, P. H.; Hennink, W. E. Physicochemical Characterization of Degradable Thermosensitive Polymeric Micelles. *Langmuir* **2004**, *20*, 9388−9395.
(74) Neradovic, D.; Van Steenbergen, M.; Vansteelant, L.; Meijer, Y.; Van Nostrum, C.; Hennink, W. Degradation Mechanism and Kinetics of Thermosensitive Polyacrylamides Containing Lactic Acid Side Chains. *Macromolecules* **2003**, *36*, 7491−7498.
(75) Kalia, J.; Raines, R. T. Hydrolytic Stability of Hydrazones and Oximes. *Angew. Chem., Int. Ed.* **2008**, *47* (39), 7523−7526.
(76) Wattiaux, R.; Laurent, N.; Wattiaux-De Coninck, S.; Jadot, M. Endosomes, Lysosomes: Their Implication in Gene Transfer. *Adv. Drug Delivery Rev.* **2000**, *41*, 201−208.

DOI: 10.1021/acsbiomaterials.5b00006
ACS Biomater. Sci. Eng. 2015, 1, 393−404